Supporting Information

Nakane et al. 10.1073/pnas.1219753110

SI Text

SI Materials and Methods

Optical Microscopy. For total internal reflection fluorescence (TIRF) microscopy, the cells were irradiated through an LF561 filter (Semrock) for red using a laser. Cell behavior was observed under a TIRF system (Olympus) using an IX71 inverted microscope (Olympus). Images were recorded with an iXon3 897 (Andor) and a PlanApo 100× TIRF objective (Olympus) using Solis software (Andor). All fluorescence images were acquired with a minimal exposure time to minimize bleaching and phototoxicity effects. All video data were analyzed by ImageJ 1.45s (http://rsb.info.nih.gov/ij/) with a plug-in particle tracker (http://www.mosaic.ethz.ch/Downloads/ParticleTracker) and macro Color FootPrint (1).

Immunolabeling of SprB on Cells. Cells were examined by immunofluorescence microscopy to identify SprB on the cell surface, as described previously (2); 100 μL of cells was put on a coverslip and chemically fixed by 3% paraformaldehyde and 0.1% glutaraldehyde in PBS for 10 min at room temperature (RT). After washing three times with PBS, the cells were blocked with 2% BSA in PBS for 10 min. After removal of the blocking solution, cells were treated with 1/1,000 dilution of antisera against SprB (3) in 2% BSA in PBS for 30 min. The cells were washed five times with PBS and treated with 1/1,000 dilution of secondary antibody conjugated to Alexa 488 (Invitrogen) or Cy3 (Sigma) in 2% BSA in PBS for 30 min. After washing five times, the coverslip was mounted on glass and observed using an inverted microscope. To stain DNA and cell membranes, 4 μM of DAPI (Invitrogen) and 2 μM of FM4-64 (Invitrogen) were used, respectively.

Measurement of the Effect of Drugs on Cell Gliding. Drug-injection experiments with gliding cells were performed by manually adding carbonyl cyanide *m*-chlorophenylhydrazone (CCCP; 10 μM) and arsenate (50 mM) in casitone yeast extract to cells in tunnel slides, as described previously (4). A series of images were taken at 1-s intervals for 30 s using phase contrast microscopy, colored with red to blue as previously described, and integrated into one image. The average area of the moving trace was calculated from 30 wild-type cells over 30 s, and the area of the moving trace for cells not treated with inhibitors was defined as 100%.

Measurement of Intracellular ATP Level. Intracellular ATP levels were measured at different times after adding CCCP (10 μM) or arsenate (50 mM) to exponentially growing cells with a standard luminescence assay using luciferase ATP-dependent light emission and ATP Bioluminescence Assay Kit HS II (Roche Applied Bioscience), as described by the manufacturer. Bioluminescence expressed in arbitrary units was measured with a DTX 800 Multimode Detector (Beckman).

Isolation of SprB-Enriched Fraction. Cells from 200 mL of culture were centrifuged at 8,000 × *g* for 10 min and suspended with PBS in one-fifth volume. The following procedures were performed at 4 °C unless otherwise noted. The suspension was mixed with 1% Triton X-100 (vol/vol) and incubated with gentle shaking for 5 min. After centrifugation at 8,000 × *g* for 10 min, the pellet was suspended in one-tenth of its original volume of PBS and then mixed with *n*-dodecyl-β-D-maltoside (dodecyl maltoside) to 1% (vol/vol). After gentle shaking for 5 min at RT, the suspension was centrifuged at 8,000 × *g* for 10 min at RT. The supernatant was fractionated by salting out with ammonium sulfate at 20% saturation, and the insoluble fraction was recovered by centrifugation at 15,000 × *g* for 15 min. The pellet was dissolved with PBS containing 1% dodecyl maltoside and used as the SprB-enriched fraction. SprB was resolved by SDS/PAGE, and gels were stained with Coomassie Brilliant Blue (CBB). The homogeneity of the fraction was estimated by densitometry of the stained gels using a GT-X970 scanner (Epson) and ImageJ 1.45s analysis software (http://rsb.info.nih.gov/ij/).

Western Blot Analysis. Western blot analysis was performed as described previously (5), with 1/3,000 dilution of antisera against SprB, GldJ, and GldK (3, 6).

Immunoprecipitation. Protein samples at the concentration of 1 μg/mL were mixed with 1/1,000 dilution of antisera against SprB, GldJ, GldK, and GldA, respectively (6–8), and incubated at 0 °C for 1 h. The protein samples were mixed with 1/30 dilution of Protein A Sepharose (GE Healthcare) and incubated at 0 °C for 1 h. The beads were washed repeatedly in PBS. After washing, the beads were suspended in Laemmli buffer and boiled at 100 °C for 10 min. Eluates were subjected to SDS/PAGE and Western blot analysis.

Electron Microscopy. For immunogold EM, the cells bound to the grid were chemically fixed using the same conditions described above and washed three times with PBS. The cells on grids were treated with 100-fold diluted antisera against the target protein in PBS containing 2% BSA and washed five times with PBS. The cells were treated with 10-fold diluted gold-labeled secondary antibody (15 nm colloidal gold-labeled goat antibody; Sigma) in PBS containing 2% BSA for 30 min at RT, washed five times, and then stained with 1% molybdate. Protein samples bound to the grid were treated with the primary antibody and washed as described above. The proteins were treated with 10-fold diluted gold-labeled secondary antibody (5 nm colloidal gold-labeled goat antibody; Sigma), washed five times, and then stained with 2% molybdate.

SI Discussion

In this text, we describe the force and torque balance of the bacterial cell on the basis of our experimental observations. The fundamental assumption of our model is that the SprB proteins run uniformly along a single helical loop track with constant speed. We consider that the frictional interactions between the SprB proteins and the substratum provide the major driving force to push the cell body forward. Note that because of the looped topology of the track, the proteins in the neighboring helical tracks are running in opposite directions. Our analysis suggests that the SprBs running toward one direction exert forces on the substratum, whereas the SprBs running toward the opposite direction are mechanically uncoupled from the substrate, so they do not hinder the net movement of the cell body. This condition, which fits our experimental observations of SprB movements, is necessary in our model to obtain cell speeds comparable with those observed experimentally. How this remarkable asymmetry in the SprB binding behavior is realized will be investigated in future studies. Our analysis also predicts that the bacterial cell body must rotate about its long axis when it translates, but the apparent pitch angle of the running SprB should remain unchanged. This result explains why the bacterial pitch angle appears to be insensitive to the translational motion of the cell body in our experiments.

When the cell is not moving with respect to the substratum, the SprB velocities with respect to that substratum may be written as $\mathbf{v}_0$ and $-\mathbf{v}_0$, respectively, where

$$\mathbf{v}_0 = \mathrm{v}_0 \sin\varphi\ \boldsymbol{e}_\theta + \mathrm{v}_0 \cos\varphi\ \boldsymbol{e}_z. \quad \textbf{[S1]}$$

Here we have defined the pitch angle of the helical track φ, and $\boldsymbol{e}_\theta$ and $\boldsymbol{e}_z$ are the unit vectors in the rotational and axial (cell's long axis) directions (Fig. S8). As SprB interacts frictionally with the substratum, the cell body may translate and rotate at the same time. The velocity of the cell body thus may be expressed as

$$\mathbf{V}_C = R\omega\ \boldsymbol{e}_\theta + V_C \boldsymbol{e}_z, \quad \textbf{[S2]}$$

where R is the radius of the cylindrical cell body and ω is the angular velocity of the cell body rotation about its long axis. SprB filaments run at the constant speed given by Eq. **S1** on the cell surface. Their velocities with respect to the substratum are

$$\mathbf{v}^{(+)} = \mathbf{V}_C + \mathbf{v}_0 \quad \text{and} \quad \mathbf{v}^{(-)} = \mathbf{V}_C - \mathbf{v}_0. \quad \textbf{[S3]}$$

Our experimental data suggest that motors powered by the proton gradient drive the movement of SprB proteins along a helical path. However, the detailed architecture of the motor–SprB complex and how it is arranged in the cell envelope currently is unknown. Therefore, we discard any effects that arise from unknown internal structures of the cell's motility machinery and instead consider that the cylindrical cell body and SprB proteins are the only mechanical units relevant to our model. Extensions of our model to more general ones will be straightforward but will involve more parameters to be determined in future experiments.

Having specified the general setup and geometry of our model, we now consider the force and torque balance conditions for the cell body and also for single SprB proteins. The motor exerts a force $f_m^{(\sigma)}$ that keeps SprB running along the helical track, where the label σ is "+" or "−", which distinguishes SprB running in different directions. SprB experiences frictional force from the substratum, which we write as $f_s^{(\sigma)}$. Assuming that this frictional force is dominated by a drag force that is proportional to the relative velocity between SprB and the substratum, we write

$$\mathbf{f}_s^{(\sigma)} = -\gamma_s^{(\sigma)} \mathbf{v}^{(\sigma)}, \quad \textbf{[S4]}$$

where $\gamma_s^{(\sigma)}$ is the friction coefficient between an SprB filament and the substratum. Because inertia of SprB is entirely neglected at this small scale, the total force acting on the SprB–motor complex must sum to zero:

$$0 = \mathbf{f}_m^{(\sigma)} + \mathbf{f}_s^{(\sigma)}. \quad \textbf{[S5]}$$

There also are force and torque balances for the cell body. The total force acting on the cell body along its translating direction (i.e., along its long axis) must be zero, which means

$$0 = -\sum_{i=1}^{N} \left(\mathbf{f}_m^{(+)} + \mathbf{f}_m^{(-)} \right) \cdot \mathbf{e}_z + (-\Gamma V_C), \quad \textbf{[S6]}$$

where Γ is the translational friction constant of the cell body. The rotational torque balance may be written as

$$0 = -\sum_{i=1}^{N} R \left(\mathbf{f}_m^{(+)} + \mathbf{f}_m^{(-)} \right) \cdot \mathbf{e}_\theta + (-\Gamma_r R\omega), \quad \textbf{[S7]}$$

where Γ_r is the rotational frictional constant of the cell body. These translational and rotational drag forces on the cell body arise mainly from frictional interactions between the cell surface and the surrounding viscous media. Plugging Eq. **S3** into Eq. **S5** and assuming uniform distribution of SprB along the looped helical track, we obtain from Eq. **S6** the cell translation velocity as

$$V_C = -\frac{N\left(\gamma_s^{(+)} - \gamma_s^{(-)}\right)}{\Gamma + N\left(\gamma_s^{(+)} + \gamma_s^{(-)}\right)} \mathrm{v}_0 \cos\varphi, \quad \textbf{[S8]}$$

where N is the number of SprB filaments running along one direction (thus the total number of SprB filaments on the cell is $2N$). Likewise, plugging Eqs. **S3**–**S5** and **S8** into Eq. **S7**, we obtain the cell rotational velocity as

$$\omega = -\frac{N\left(\gamma_s^{(+)} - \gamma_s^{(-)}\right)}{\Gamma_r + N\left(\gamma_s^{(+)} + \gamma_s^{(-)}\right)R} \mathrm{v}_0 \sin\varphi. \quad \textbf{[S9]}$$

As can be seen clearly from Eqs. **S8** and **S9**, the cell does not translate or rotate when the SprB filaments traveling in both directions contribute equally to the force generation of the cell. We then study the case in which only SprB filaments running toward the "−" (negative z) direction contribute to the force generation of the cell. This situation may be described by setting $\gamma_s^{(+)} = 0$ in the above results. In this case, the cell body translates along the "+" (positive z) direction and, at the same time, rotates counterclockwise along its progressing direction. In this strongly asymmetric case, we obtain from Eqs. **S8** and **S9**

$$V_C = \frac{N\gamma_s}{\Gamma + N\gamma_s} \mathrm{v}_0 \cos\varphi \quad \textbf{[S10]}$$

and

$$\omega = \frac{N\gamma_s}{\Gamma_r + N\gamma_s R} \mathrm{v}_0 \sin\varphi, \quad \textbf{[S11]}$$

where we have used the shorthand notation $\gamma_s^{(-)} = \gamma_s$. In the laboratory frame, the apparent velocities of the SprBs are obtained from Eq. **S3** as

$$\mathbf{v}^{(+)} = (1+\alpha_\omega)\ \mathrm{v}_0 \sin\varphi\ \boldsymbol{e}_\theta + (1+\alpha_v)\ \mathrm{v}_0 \cos\varphi\ \boldsymbol{e}_z \quad \textbf{[S12]}$$

and

$$\mathbf{v}^{(-)} = -(1-\alpha_\omega)\ \mathrm{v}_0 \sin\varphi\ \boldsymbol{e}_\theta - (1-\alpha_v)\ \mathrm{v}_0 \cos\varphi\ \boldsymbol{e}_z, \quad \textbf{[S13]}$$

where we have defined

$$\alpha_v = \frac{N\gamma_s}{\Gamma + N\gamma_s} \quad \text{and} \quad \alpha_\omega = \frac{N\gamma_s R}{\Gamma_r + N\gamma_s R}. \quad \textbf{[S14]}$$

Our observations suggest that there are sufficient SprB proteins on a cell, so we may expect $N\gamma_s \gg \Gamma$ and Γ_r, i.e., $\alpha_v \approx 1$ and $\alpha_\omega \approx 1$, which lead to

$$V_C \simeq \mathrm{v}_0 \cos\varphi \quad \textbf{[S15]}$$

and

$$\omega \simeq \frac{\mathrm{v}_0 \sin\varphi}{R}. \quad \textbf{[S16]}$$

In this strong anchoring limit, the motions of the cell body and the protein become purely geometric; the SprB filaments adhere to

the substratum, and the cell body is pushed forward at a speed equal to the freely moving SprB. This limiting case is indeed close to what we have observed in our experiments, and we can conclude that the strongly asymmetric binding of SprB proteins should be realized for *Flavobacterium johnsoniae* studied here. (The physical model to explain how the asymmetric cooperative binding/unbinding dynamics can arise from the simple helical geometry will be published separately in future.)

In this limit, the apparent velocities of the SprB filaments become

$$\mathbf{v}^{(+)} = 2v_0 \sin\varphi\, \boldsymbol{e}_\theta + 2v_0 \cos\varphi\, \boldsymbol{e}_z \quad \text{and} \quad \mathbf{v}^{(-)} = 0. \qquad \textbf{[S17]}$$

Thus, the moving SprB filaments ("+" ones in this case) move twice as fast as the cell body, but the apparent pitch angle does not change and remains at the original value φ, which is consistent with our experimental observations.

1. Uenoyama A, Miyata M (2005) Gliding ghosts of Mycoplasma mobile. *Proc Natl Acad Sci USA* 102(36):12754–12758.
2. Nakane D, Miyata M (2007) Cytoskeletal "jellyfish" structure of Mycoplasma mobile. *Proc Natl Acad Sci USA* 104(49):19518–19523.
3. Nelson SS, Bollampalli S, McBride MJ (2008) SprB is a cell surface component of the Flavobacterium johnsoniae gliding motility machinery. *J Bacteriol* 190(8):2851–2857.
4. Nakane D, Miyata M (2012) Mycoplasma mobile cells elongated by detergent and their pivoting movements in gliding. *J Bacteriol* 194(1):122–130.
5. Sato K, et al. (2010) A protein secretion system linked to bacteroidete gliding motility and pathogenesis. *Proc Natl Acad Sci USA* 107(1):276–281.
6. Braun TF, McBride MJ (2005) Flavobacterium johnsoniae GldJ is a lipoprotein that is required for gliding motility. *J Bacteriol* 187(8):2628–2637.
7. Agarwal S, Hunnicutt DW, McBride MJ (1997) Cloning and characterization of the Flavobacterium johnsoniae (Cytophaga johnsonae) gliding motility gene, gldA. *Proc Natl Acad Sci USA* 94(22):12139–12144.
8. Rhodes RG, Nelson SS, Pochiraju S, McBride MJ (2011) Flavobacterium johnsoniae sprB is part of an operon spanning the additional gliding motility genes sprC, sprD, and sprF. *J Bacteriol* 193(3):599–610.

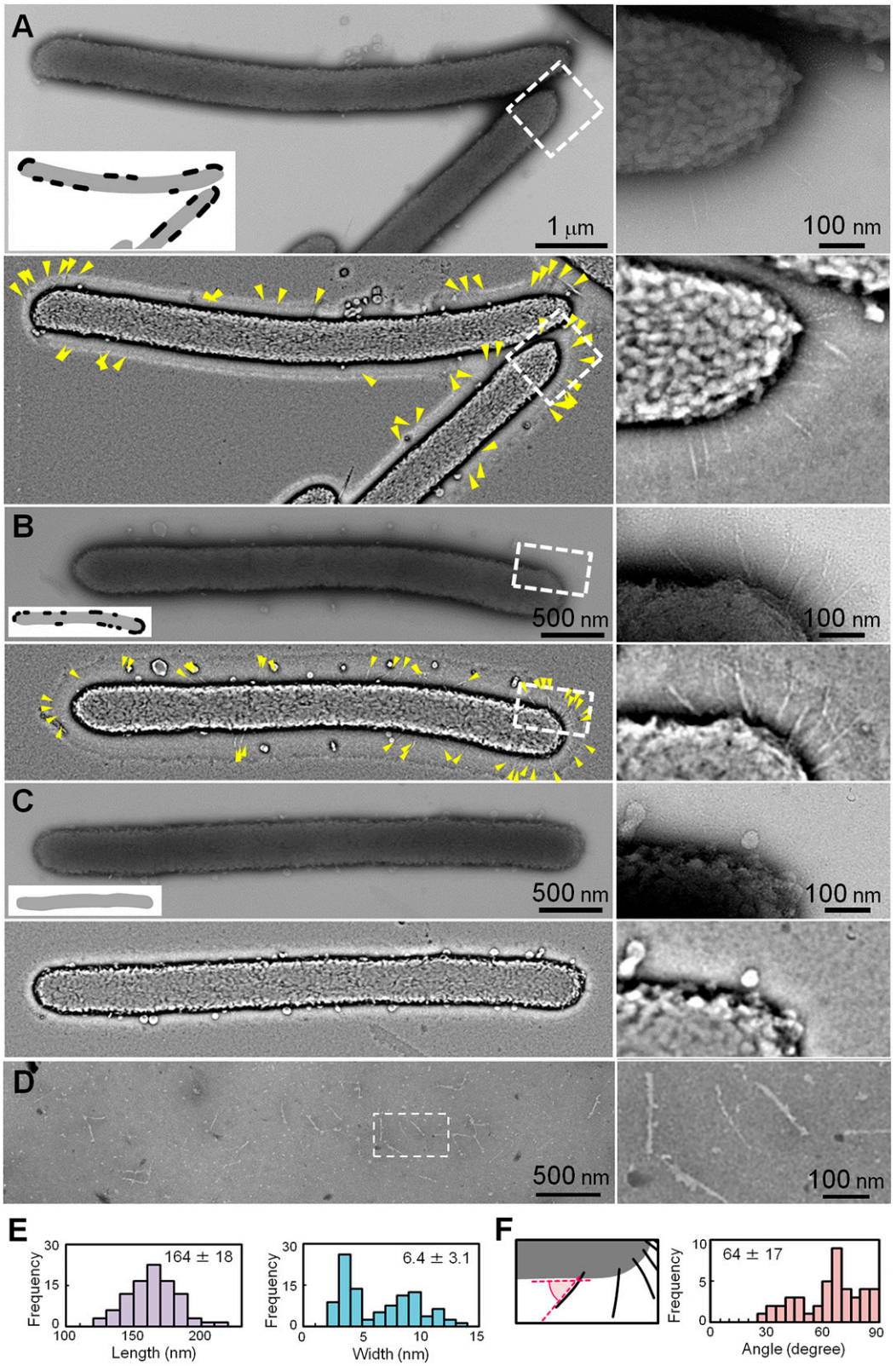

Fig. S1. Filamentous structures observed by EM with negative staining. (*A* and *B*) Wild-type *F. johnsoniae* CJ1827 (*A*) and UW101 (*B*). (*C*) *sprB* deletion mutant CJ1922. In *A*–*C*, the upper images are the originals and the lower images are bandpass filtered to visualize the surface filaments clearly. Yellow triangles indicate the filamentous structure extending from the outer membrane. (*A*–*C Insets*) Surface regions exhibiting filaments, indicated in black. (*D*) SprB-enriched fraction. The dashed box region is magnified and presented in the right part of each image (*A*–*D*). (*E*) Distribution of the length (*Left*) and width (*Right*) of the isolated SprB filaments. The average length and width from 80 filaments are shown. (*F*) Distribution of the angle between outer membrane and SprB filaments on cells. (*Left*) Measured angle; (*Right*) distribution of the angles from 45 filaments and the average angle.

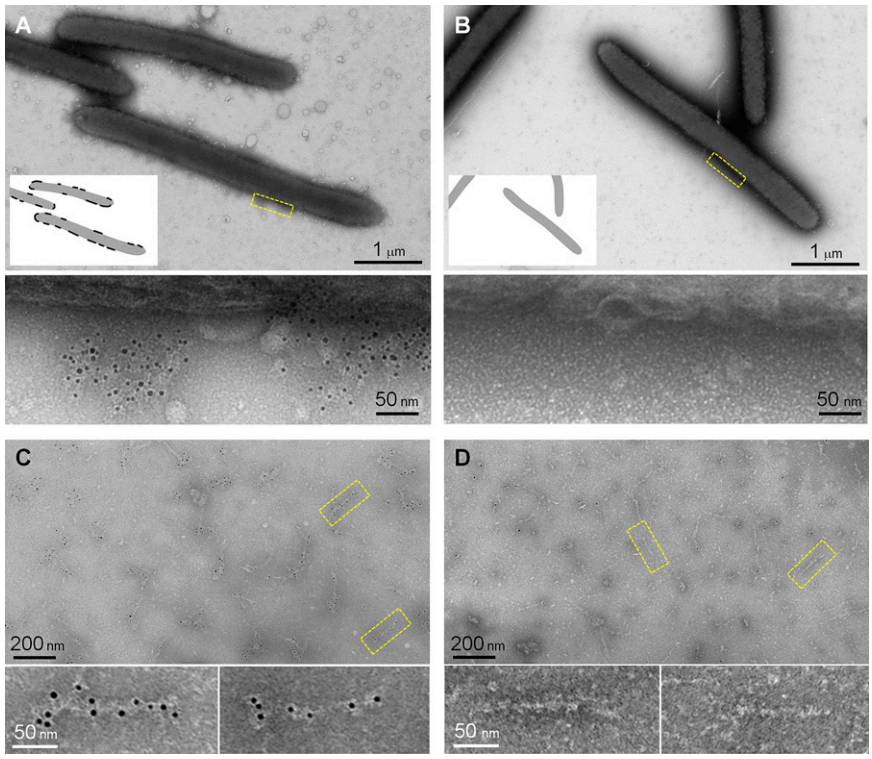

Fig. S2. Immunogold EM. (*A* and *B*) Negative staining of the wild-type (*A*) and *sprB* deletion mutant cells (*B*). The cells were chemically fixed and labeled with antisera against SprB and 5-nm colloidal gold. The dashed box region is magnified and presented in the lower part of each image. (*Insets*) Surface regions with gold clusters, indicated in black. (*C* and *D*) Negative staining of the SprB-enriched cell fraction. The proteins were labeled with antisera against SprB (*C*) and GldJ (*D*), and 5-nm colloidal gold. Dashed box regions are magnified and presented at bottom.

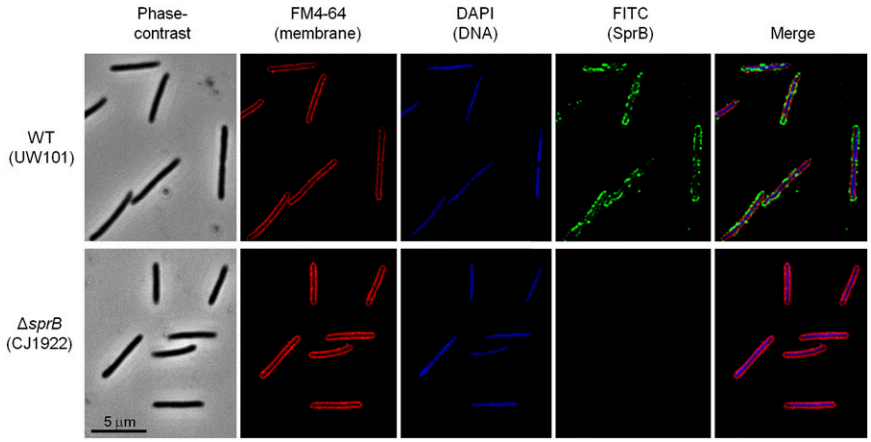

Fig. S3. Localization of SprB. The wild-type (WT) and *sprB* deletion mutant (CJ1922) cells were chemically fixed with 3% paraformaldehyde and 0.3% glutaraldehyde. Cell membrane, DNA, and SprB were labeled with FM4-64 (red), DAPI (blue), and antisera against SprB plus anti-rabbit IgG-FITC (green), respectively, as described in *Materials and Methods*.

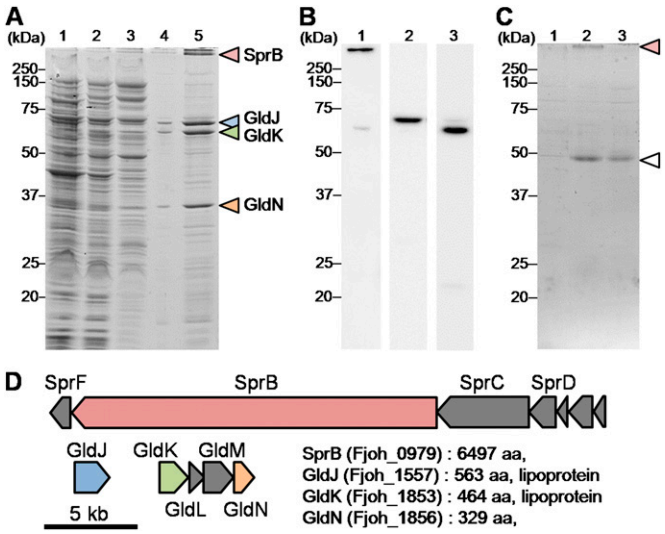

Fig. S4. Partial purification of SprB. (*A*) Protein profiles of fractions in the purification procedure. The protein fractions were applied to SDS-12.5% PAGE and subjected to CBB staining (lanes 1–5). Lane: 1, whole cell lysate; 2, Triton X-100-insoluble fraction; 3, dodecyl maltoside-soluble fraction; 4, precipitate with 20% saturated ammonium sulfate; 5, concentrated fraction from the sample in lane 4. Molecular masses are indicated on the left. The protein bands of SprB, GldJ, GldK, and GldN are marked by triangles, respectively. (*B*) Immunoblots using antisera against SprB (lane 1), GldJ (lane 2), and GldK (lane3), respectively. (*C*) Immunoprecipitation using antisera against SprB (lane 2) and GldA (lane 3), and without antisera (lane 1). Red and white triangles indicate the bands of SprB and albumin, respectively. (*D*) Genes encoding proteins found in the SprB-enriched ammonium sulfate precipitation fraction.

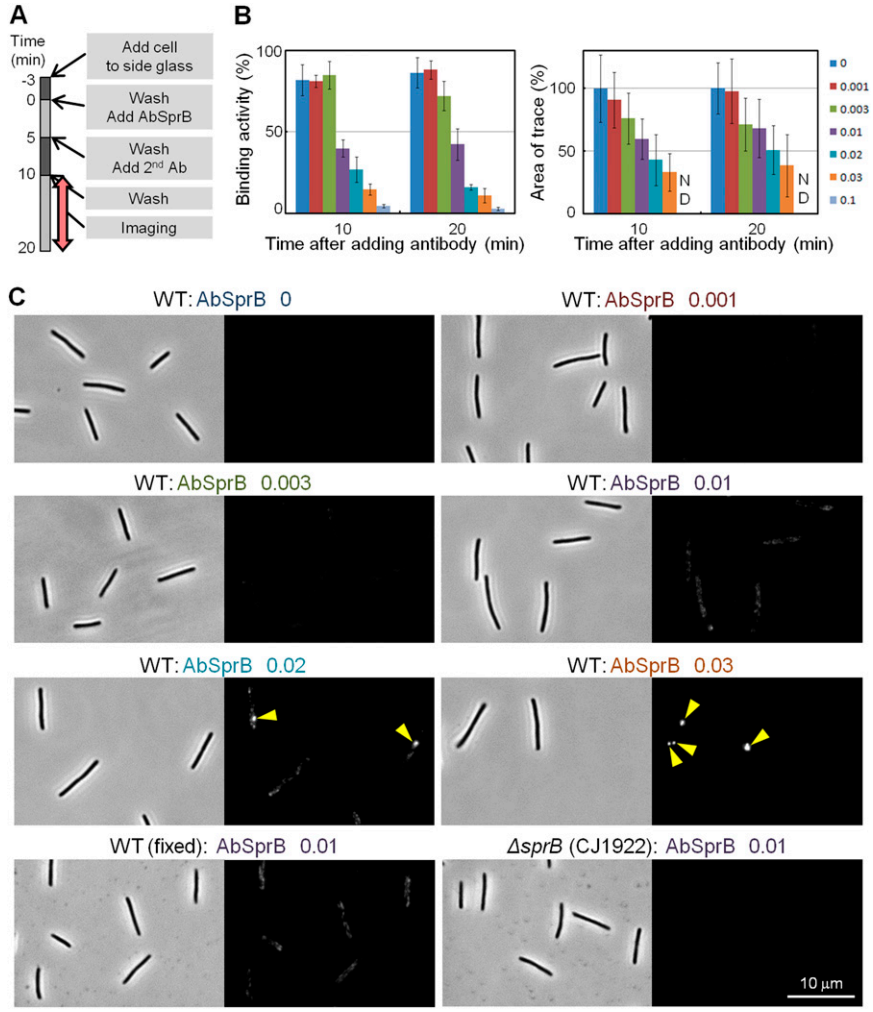

Fig. S5. Immunofluorescence microscopy in a living cell. (*A*) Scheme of experimental procedure. Cells were poured into a tunnel slide and incubated for 3 min. After removing floating cells with fresh medium, anti-SprB antiserum was added to the slide and incubated for 5 min. After washing with fresh medium, secondary antibody was added and incubated for 5 min. After washing with fresh medium, the slide was used for the imaging experiment. The observation was done in 10 min. Time was indicated as 0 when antiserum was added. (*B*) Binding and gliding activity after adding anti-SprB antiserum. For binding activity, the number of cells in 223 × 166 μm was measured at each time point. The number at time 0 is defined as 100%. For gliding activity, the area of trace for 30 s at each time point was measured. The averages from 30 individual cell traces are shown. All experiments were performed three times. (*C*) Fluorescence signal detected from a living cell. (*Left*) Phase-contrast images. (*Right*) Epifluorescence images. The concentration of anti-SprB antiserum used is presented in each panel. Yellow arrowheads indicate strong signals due to aggregation of SprB and antibody.

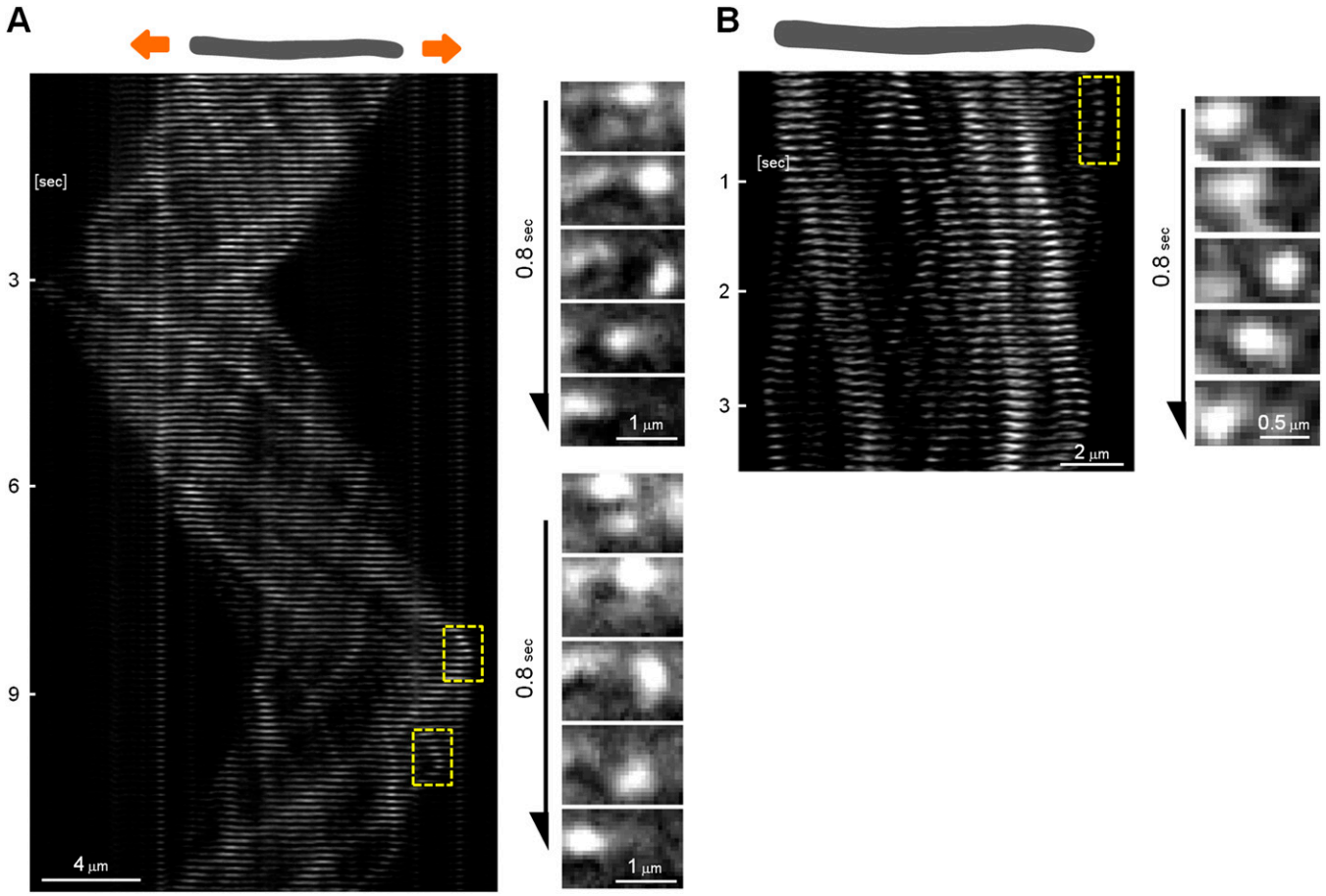

Fig. S6. SprB motion in a translocating cell (*A*) and in a nontranslocating cell (*B*). (*Left*) Kymograph of SprB signals. The *x*-axis is the position of SprB signals with respect to the substratum (glass), and the *y*-axis is time. A series of images were recorded at 0.1-s intervals. The positions of the cells at 0 s is illustrated in the cartoons at the top. (*Right*) Montage of looping motion of SprB signals observed at the cell poles. The regions shown correspond to the dashed yellow boxes in the kymographs.

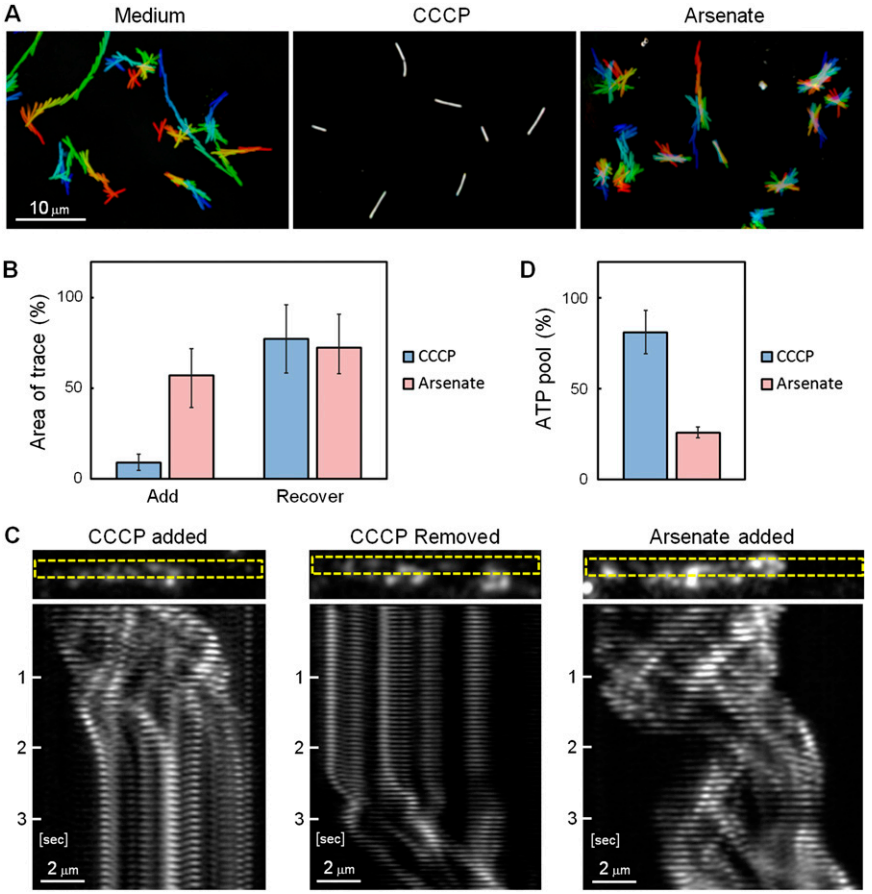

Fig. S7. Effects of various inhibitors on the gliding motility and helical loop-like motion of SprB. (*A*) Moving trace of wild-type cells. The inhibitors CCCP and arsenate were added to cells in tunnel slides (*Materials and Methods*). After a 10-min incubation, a series of images were taken every 1 s for 30 s, colored from red (time 0), to yellow, green, and finally blue (30 s), and integrated into one image. (*B*) Effect of inhibitors on gliding activity. The area of moving trace for 30 s was measured 10 min after addition of inhibitors, then 10 min after removal of inhibitors by replacement with fresh medium. The average area of moving trace with SD was calculated from 30 cells, and the area of the wild-type cells without treatment at time 0 for 30 s was defined as 100%. (*C*) Kymographs of SprB signals for cells treated with the inhibitors. SprB motion was examined immediately after addition or removal of inhibitors. Location of SprB on the cell surface at time 0 is shown in the boxes above the kymographs. The yellow dashed regions in the boxes were used for making the kymographs. The *x*-axis is the position of SprB signals with respect to the substratum (glass), and the *y*-axis is time. The kymographs for CCCP added and CCCP removed come from Movies S7 and S8, respectively. (*D*) Effect of inhibitors on intracellular ATP levels. The intracellular ATP levels after 10 min of treatment with CCCP or arsenate were measured by luminescence assay. The bioluminescence value of nontreated cells was defined as 100%.

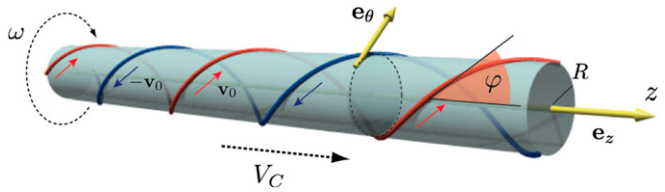

Fig. S8. Mechanical model of *Flavobacterium* gliding motility. Note that we take a (nonstandard) left-handed coordinate system to fit the left-handed helical geometry of the track. In the calculations, we consider the case in which the cell body moves toward the positive *z* direction and rotates counterclockwise along its progressing direction. In this case, both V_C *and* ω are positive. For more details, see *SI Text*.

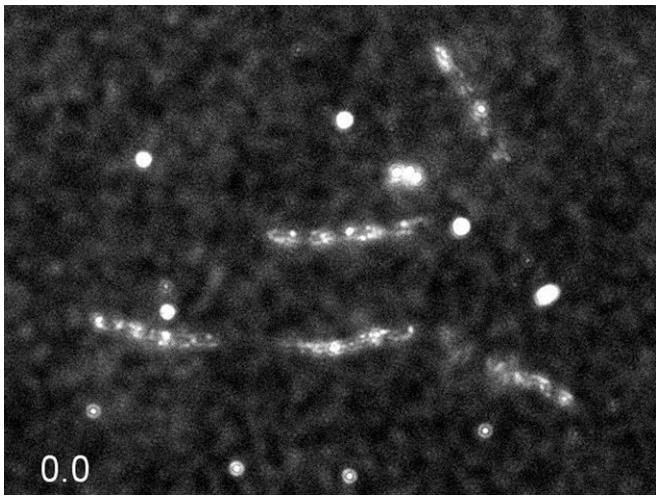

Movie S1. Dynamics of the surface protein SprB (field image). Images were recorded at 0.1-s intervals for 9 s by epifluorescence microscopy. Time is shown at bottom left. Area: 40 × 30 μm.

Movie S1

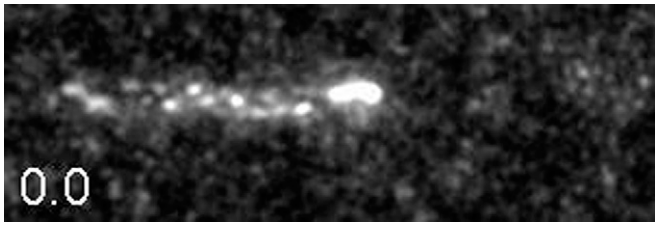

Movie S2. Dynamics of SprB in a translocating cell. Images were recorded at 0.1-s intervals for 4 s by epifluorescence microscopy. Time is shown at bottom left. Area: 18.8× 6.3μm. The images in Fig. 2 come from this movie.

Movie S2

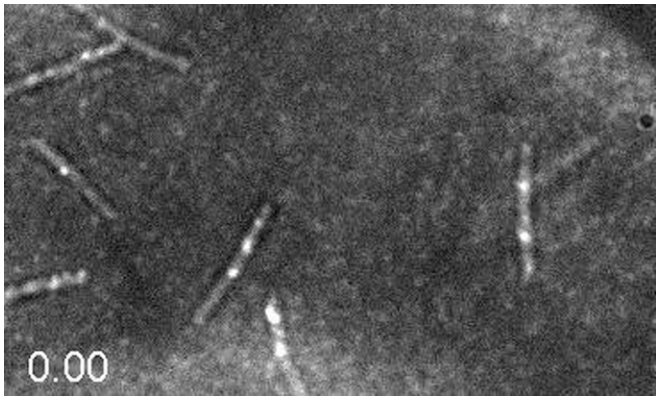

Movie S3. Left-handed helical flow of SprB (field image). Images were recorded at 0.05-s intervals for 10 s under TIRF microscopy. Outlines of cells were visualized by weak illumination using a halogen lamp. Time is shown at bottom left. Area: 37× 22 μm.

Movie S3

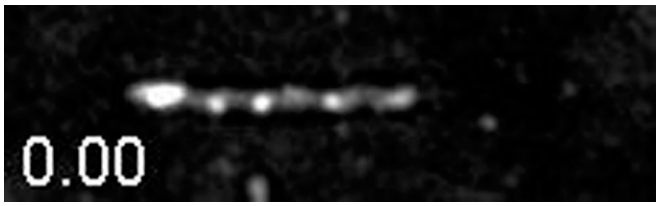

Movie S4. Left-handed helical flow of SprB in a translocating cell. Images were recorded over a 2-s period at 0.05-s intervals under TIRF microscopy. Outlines of cells were visualized by weak illumination using a halogen lamp. Time is shown at bottom left. Area: 20 × 6 μm. The images in Fig. 3 come from this movie.

Movie S4

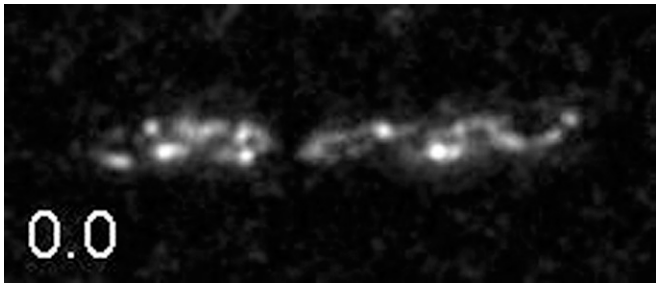

Movie S5. Dynamics of SprB in a nontranslocating cell. Images were recorded at 0.1-s intervals for 4 s by epifluorescence microscopy. Time is shown at bottom left. Area: 14.6× 6.3 μm. The images in Fig. 4*A* come from this movie.

Movie S5

Movie S6. Left-handed helical flow of SprB in a nontranslocating cell. Images were recorded at 0.05-s intervals for 2 s under TIRF microscopy. Outlines of cells were visualized by weak illumination using a halogen lamp. Time is shown at bottom left. Area: 20 × 6 μm. The images in Fig. 4*B* come from this movie.

Movie S6

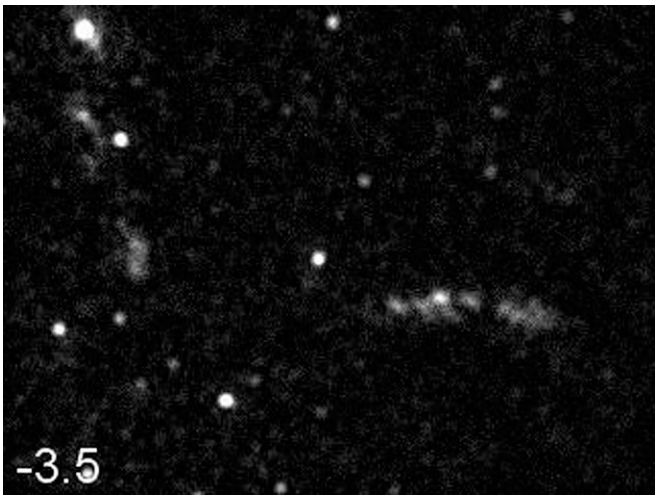

Movie S7. Effect of CCCP (added immediately before examination) on movement of SprB. Images were recorded at 0.05-s intervals for 12 s by epifluorescence microscopy. Time is shown at bottom left. Area: 20× 15 μm. An image in Fig. S7*C* comes from this movie.

Movie S7

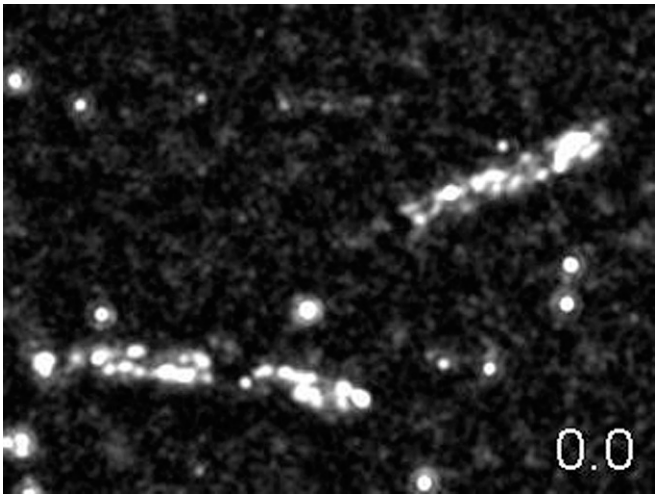

Movie S8. Movement of SprB commences within seconds of removal of CCCP. Images were recorded at 0.1-s intervals for 15 s by epifluorescence microscopy. Time is shown at bottom right. Area: 20× 15 μm. An image in Fig. S7*C* comes from this movie.

Movie S8

Movie S9. Animation of the helical loop track model for *Flavobacterium* gliding motility.

Movie S9